J Electr Eng Technol Vol. 9, No. 5: 1746-1752, 2014
http://dx.doi.org/10.5370/JEET.2014.9.5.1746

ISSN(Print) 1975-0102
ISSN(Online) 2093-7423

An Application of Proportional-Resonant Controller in MMC-HVDC System under Unbalanced Voltage Conditions

Ngoc-Thinh Quach*, Ji-Han Ko, Dong-Wan Kim** and Eel-Hwan Kim†**

Abstract – This paper presents an application of proportional-resonant (PR) current controllers in modular multilevel converter-high voltage direct current (MMC-HVDC) system under unbalanced voltage conditions. The ac currents are transformed and controlled in the stationary reference frame (αβ-frame). Thus, the complex analysis of the positive and negative sequence components in the synchronous rotating reference frame (dq-frame) is not necessary. With this control method, the ac currents are kept balanced and the dc-link voltage is constant under the unbalanced voltage fault conditions. The simulation results based on a detailed PSCAD/EMTDC model confirm the effectiveness of the proposed control method.

Keywords: Integral-proportional controller, Modular multilevel converter-high voltage direct current system, Negative sequence component, Proportional-resonant controller, Unbalanced voltage conditions

1. Introduction

The modular multilevel converter (MMC)-based high voltage direct current (HVDC) system is a new type of voltage source converter (VSC) for medium or high voltage direct current power transmission. Recently, it has become more competitive because it has advantages over normal VSC-HVDC system such as low total harmonic distortion, high efficiency, and high capacity [1, 2]. The operation of the MMC-HVDC system has been investigated by many authors over the world. In [3-5], the authors presented the control strategies for eliminating the circulating currents and maintaining the capacitor voltage balancing of the MMC. The dynamic performances of the MMC-HVDC system have been analyzed in [6]. Similar to other HVDC systems, the stable and reliable operation of the system must be researched carefully, especially when the system operates under fault conditions. In [6-8], the authors showed out the control methods of the MMC-HVDC system under the unbalanced voltage conditions. Almost all of them only focus on the use of proportional-integral (PI) current controllers in the synchronous rotating reference frame (dq-frame) for enforcing steady-state error to zero. However, the use of these PI current controllers will be difficult under the unbalanced voltage conditions because of the complex control of the positive and negative sequence components of the currents [6-8]. Recently, the simple proportional-resonant (PR) current controllers in the stationary reference frame (αβ-frame) have been developed to overcome this problem [10]. The most important performance of the PR current controllers is that the currents are controlled directly in the αβ-frame. Therefore, the complicated analysis of the positive and negative sequence components of the currents is ignored.

This paper presents an application of the PR current controllers in the MMC-HVDC system under the unbalanced voltage conditions. The complicated analysis of the positive and negative sequence components in the dq-frame is not necessary because the currents are controlled directly in the αβ-frame. The purposes are to keep a balance on the ac currents and a constant on the dc-link voltage.

The rest of this paper is organized as follows. Section 2 is the configuration of the MMC-HVDC system. The proposed control method of the MMC-HVDC system is presented in Section 3. Section 4 is the simulation results. Finally, Section 5 draws the conclusions.

2. Configuration of the MMC-HVDC System

The configuration of the MMC-HVDC system is depicted in Fig. 1. A MMC-HVDC system consists of two back-to-back-connected MMC units. Each MMC is structured by six arms as shown in Fig. 1(b). Each arm has a total of N sub-modules (SM) connected in series and a series inductor which provides current control within the phase arms and limits fault currents. Two arms in the same leg comprise a phase unit. A SM is a half-bridge cell which consists of two IGBTs, two anti-parallel diodes, and a capacitor. The ac-side of each MMC is connected to a unity grid through a series-connected resistance and inductance and a wye-delta three-phase transformer.

The output voltage of each SM, v_{sm}, has two values: (i) $v_{sm} = v_c$ if T_1 is switched on and T_2 is switched off, (ii) v_{sm}

† Corresponding Author: Dept. of Electrical Engineering, Jeju National University, S. Korea. (ehkim@jejunu.ac.kr)
* Dept. of Electrical Engineering, Jeju National University, S. Korea. (ngoct1984@yahoo.com)
** Multidisciplinary Graduate School Program for Wind Energy, Jeju National University, S. Korea. ({Jhon-e, segi305}@naver.com)
Received: October 4, 2013; Accepted: April 7, 2014

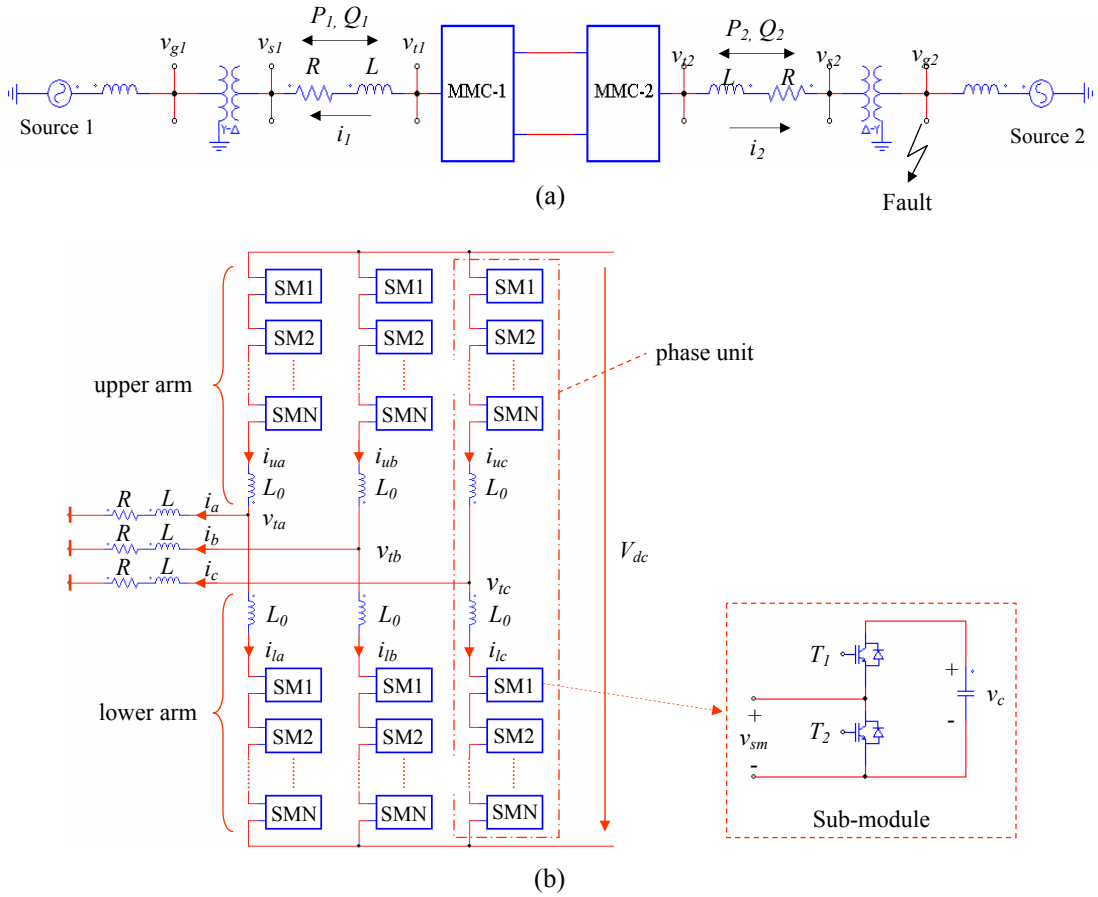

Fig. 1. Configuration of the MMC-HVDC system: (a) single-line diagram; (b) circuit configuration

= 0 if T_1 is switched off and T_2 is switched on. The charging or discharging of the capacitor depends on the direction of the current. If the current flows into the SM, the capacitor is charged. If the current flows out of the SM, the capacitor is discharged.

3. The Proposed Control Method of the MMC-HVDC System

3.1 Proportional-resonant controller

The PR controller has been analyzed in [10]. A PR controller is constituted by the proportional regulator and resonant controller. The transfer function of the ideal PR controller with an infinite gain at the ac frequency of ω is given by

$$G = K_p + \frac{K_i s}{s^2 + \omega^2} \quad (1)$$

The K_p is the proportional gain that is adjusted as the same way for a PI controller. The K_i can be tuned for shifting the magnitude response vertically. Bode plots of the PR controller are shown in Fig. 2. As mentioned before, the magnitude is infinite at the resonant frequency, this is necessary to enforce the steady-state error to zero. The magnitude response of the PR controller is increasing with the increase of the value of K_p (Fig. 2(a)). A small K_i gives a low resonant peak, whereas a large K_i gives a higher resonant peak (Fig. 2(b)).

The advantage of the PR controller is that it can control directly signals in the αβ-frame. Hence, a transformation into the dq-frame is not necessary. This is very important in case of the unbalanced voltage conditions. Because the signals in the αβ-frame only have one component with the frequency of ω, the analysis of the positive and negative components under the unbalanced voltages is thus ignored. As a result, the control system with the PR controller will be more simple than that with the PI controller.

3.2 The current controllers

Under the unbalanced voltage conditions, the conventional method is to analyze the positive and negative sequence components in the dq-frame [6-9]. The transformation between the positive $(dq)^+$, negative $(dq)^-$ and αβ-frames are given by [9].

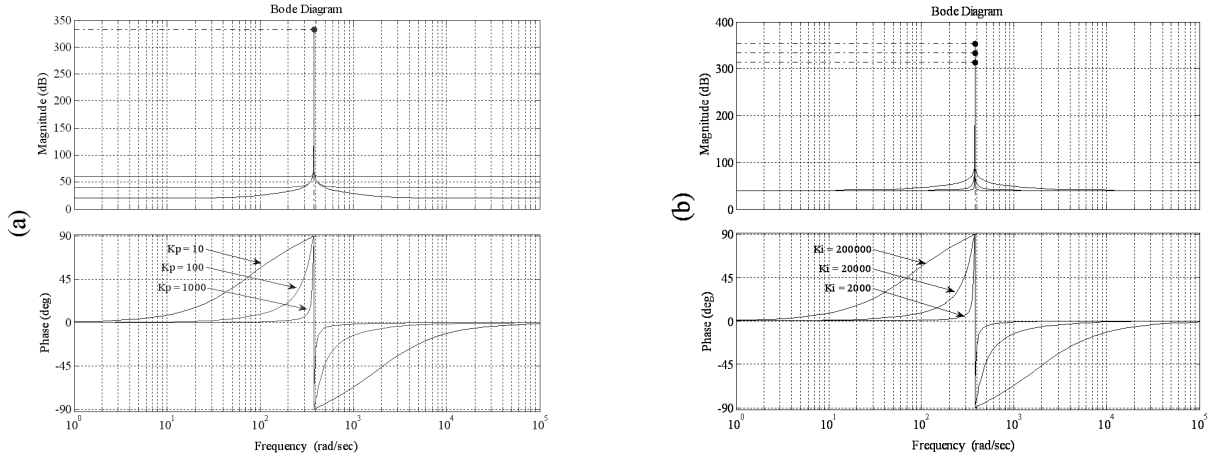

Fig. 2. Bode plots of the PR controller: (a) Changing K_p and Fixing K_i; (b) Fixing K_p and Changing K_i

$$F_{dq}^{+} = F_{\alpha\beta}.e^{-j\theta} \qquad F_{dq}^{-} = F_{\alpha\beta}.e^{j\theta}$$
$$F_{dq}^{+} = F_{dq}^{-}.e^{-j2\theta} \qquad F_{dq}^{-} = F_{dq}^{+}.e^{j2\theta} \tag{3}$$

where $\theta=\omega t$. F denotes the vector of the voltage and current. Superscripts + and - refer to the positive $(dq)^{+}$ and negative $(dq)^{-}$ -frames, respectively.

However, this control method is complicated and it requires more current controllers due to the negative sequence components. A more simple method is to analyze the operation of the system in the αβ-frame because there is only one component with the frequency of ω in the αβ-frame under the unbalanced voltage conditions. From Fig. 1(b), the ac-side phase voltages are calculated by

$$v_{sk\_j} = i_{k\_j}R + L\frac{di_{k\_j}}{dt} + v_{tk\_j} \tag{4}$$

where j is the three-phase components of the voltages or currents, $j = a, b, c$. k denotes to the MMC-1 and MMC-2, $k = 1, 2$. v_{sk_j}, v_{tk_j}, and i_{k_j} are the three-phase voltages and currents of the MMC-k. R and L are the resistance and inductance of the system, respectively.

These voltages can be rewritten in the αβ-frame as

$$v_{sk\_\alpha} = i_{k\_\alpha}R + L\frac{di_{k\_\alpha}}{dt} + v_{tk\_\alpha} \tag{5}$$

$$v_{sk\_\beta} = i_{k\_\beta}R + L\frac{di_{k\_\beta}}{dt} + v_{tk\_\beta} \tag{6}$$

where v_{sk_α}, v_{sk_β}, v_{tk_α}, v_{tk_β}, i_{k_α} and i_{k_β} are the αβ-axis components of the three-phase voltages and currents of the MMC-k.

From (5) and (6), the PWM voltages can be calculated as

$$v_{tk\_\alpha} = -i_{k\_\alpha}R - L\frac{di_{k\_\alpha}}{dt} + v_{sk\_\alpha} \tag{7}$$

(2)
$$v_{tk\_\beta} = -i_{k\_\beta}R - L\frac{di_{k\_\beta}}{dt} + v_{sk\_\beta} \tag{8}$$

The PWM voltages will depend on the control of the ac currents. The current controllers used in this paper are the PR current controllers. The α-axis current is used to control the reactive power, meanwhile the β-axis current is employed to control the active power or the dc-link voltage. The current controllers can be described as

$$v_{tk\_\alpha}^{*} = -\left(K_p + \frac{K_i s}{s^2+\omega^2}\right)\left(i_{k\_\alpha}^{*} - i_{k\_\alpha}\right) + v_{sk\_\alpha} \tag{9}$$

$$v_{tk\_\beta}^{*} = -\left(K_p + \frac{K_i s}{s^2+\omega^2}\right)\left(i_{k\_\beta}^{*} - i_{k\_\beta}\right) + v_{sk\_\beta} \tag{10}$$

where the superscript * denotes the reference values of the signals.

Assuming that the three-phase currents are kept in balance under the unbalanced voltage conditions with the PR current controllers. Therefore, the negative sequence component of the currents is zero. The instantaneous power at the ac-side can be expressed by

$$P_k = \frac{3}{2}\left(v_{sk\_d}^{+}.i_{k\_d} + v_{sk\_q}^{+}.i_{k\_q}\right) \tag{11}$$

$$Q_k = \frac{3}{2}\left(v_{sk\_d}^{+}.i_{k\_q} - v_{sk\_q}^{+}.i_{k\_d}\right) \tag{12}$$

where P and Q are the active and reactive powers at the ac-side, respectively. $v_{sk\_d}^{+}$ and $v_{sk\_q}^{+}$ are the dq-axis components of the voltages in the positive $(dq)^{+}$-frame.

Because $v_{sk\_d}^{+} = 0$, the reference currents in dq-frame can be rewritten as

$$i_{k\_q}^{*} = \frac{2}{3}\frac{P_k^{*}}{v_{sk\_q}^{+}} \tag{13}$$

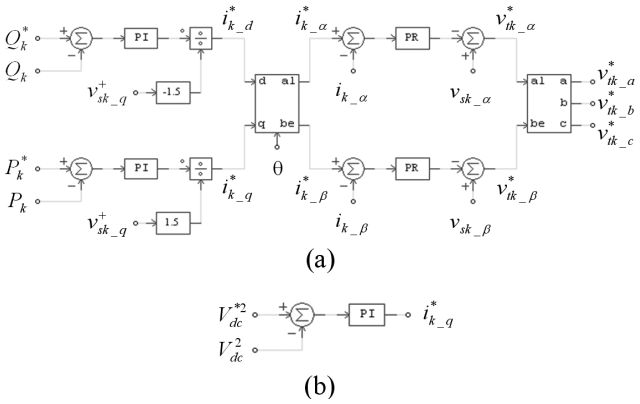

(a)

(b)

Fig. 3. Overall control diagram of the MMC-HVDC system

$$i_{k\_d}^{*} = -\frac{2}{3}\frac{Q_k^{*}}{v_{sk\_q}^{+}} \tag{14}$$

If the MMC-*k* is used to control the dc-link voltage, the q-axis component of the reference current is modified by [6, 7]

$$i_{k\_q}^{*} = \left(K_p + \frac{K_i}{s}\right)\left(V_{dc}^{*2} - V_{dc}^{2}\right) \tag{15}$$

where V_{dc} is the dc-link voltage. The band stop filter can be used to filter the double frequency oscillation component in the dc-link voltage.

Finally, these current components are transformed into the αβ-frame by using (2) to get the reference currents for (9) and (10).

The overall control diagram of the MMC-HVDC system is shown in Fig. 3. The outer control loop is employed to control the active power, the reactive power and dc-link voltage with the PI controllers. The output signals of the outer control loop are the reference currents in the dq-frame, and these currents are then transformed into the αβ-frame. The inner control loop is used to control the currents with the PR current controllers. The output signals of the inner control loop are the reference voltages that are applied to the PWM method and the capacitor voltage balancing method to get the gating signals for IGBTs. The q-axis current component of the MMC-*k* in Fig. 3(a) will be replaced by the Fig. 3(b) if the MMC-*k* is used to control the dc-link voltage.

4. Simulation results

To evaluate the effectiveness of the proposed control methods, the simulation results are carried out in two cases with the support of the PSCAD/EMTDC model. The first case is the control of the MMC-HVDC system under single phase-to-ground (SPG) fault with the PI current controllers and without compensating the negative sequence component of the currents. Another case is the use of the proposed control method for the MMC-HVDC system under the same fault as the first case. The parameters of the MMC-HVDC system are shown in Table 1. The MMC-1 is used to control the dc-link voltage and the reactive power, meanwhile the MMC-2 is used to control the active and reactive powers. In the case of study, the command active power is set at 200 MW and it is flowing from the MMC-1 to the MMC-2. The command reactive power is zero at

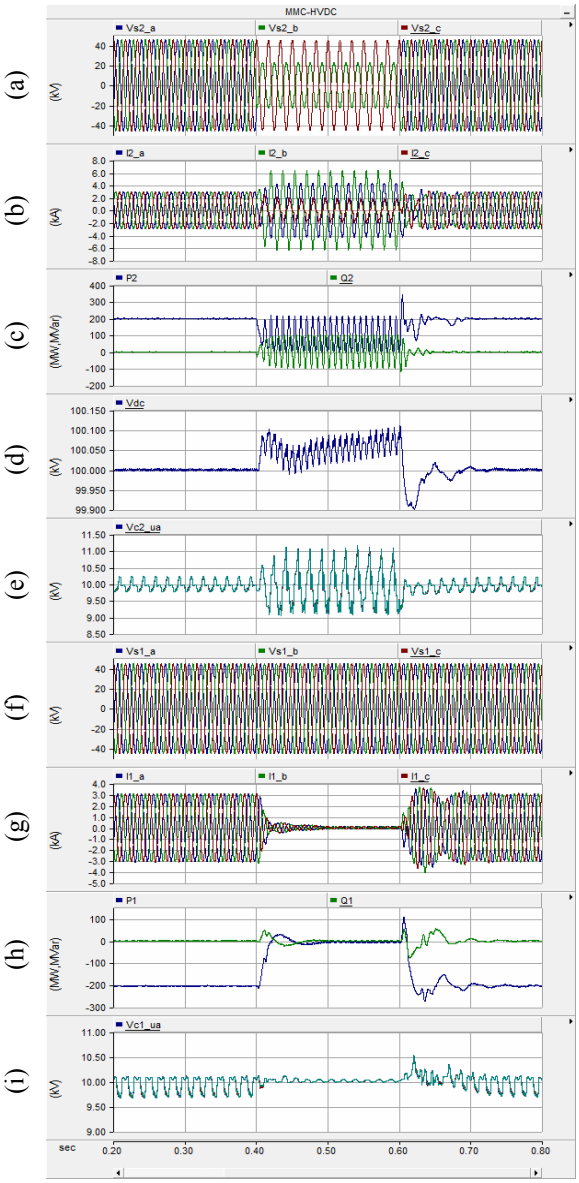

Fig. 4. The operation of the MMC-HVDC system with the PI current controllers and without compensating the negative sequence component of the currents under the single phase-to-ground fault: (a) MMC-2 three-phase voltages; (b) MMC-2 three-phase currents; (c) MMC-2 active and reactive powers; (d) dc-link voltage; (e) MMC-2 capacitor voltages; (f) MMC-1 three-phase voltages; (g) MMC-1 three-phase currents; (h) MMC-1 active and reactive powers; (i) MMC-1 capacitor voltages.

both MMC. The SPG fault on the ac-side of the MMC-2 occurs at t = 0.4 s and removes at t = 0.6 s. The simulation results in two cases are described in Fig. 4 and Fig. 5, respectively.

From t = 0.2 s to t = 0.4 s, the operation of the MMC-HVDC system in the steady-state in two cases are almost the same. However, it is quite different when the system operates under the SPG fault. Figs. 4(a) and Fig. 5(a) show the three-phase voltages of the MMC-2. The three-phase currents of the MMC-2 are presented in Fig. 4(b) and Fig. 5(b). It can be seen that the currents are not balanced without compensating the negative sequence component of the currents (Fig. 4(b)). With the PR controller, it compensates both positive and negative sequence components. Therefore, the three-phase currents are balanced as depicted in Fig. 5(b). In this case, the currents are controlled up to the rating value to achieve the maximum power. Because the fault occurs at the ac-side of the MMC-2, the active power received at the MMC-2 decreases and there is no oscillation in the power with the PR current controllers (Fig. 5(c)). Meanwhile, there is a large oscillation in the power with the PI current controllers (Fig. 4(c)).

By using the proposed control method, the dc-link voltage is almost controlled at the reference value as shown in Fig. 5(d). Figs. 4(e) and Fig. 5(e) depict the capacitor voltages of the upper arm of phase-a in two cases, respectively. Besides, the three-phase voltages and currents of the MMC-1 are also shown in Figs. 4(f)-(g) and Figs. 5(f)-(g). The active and reactive powers of the MMC-1 are depicted in Fig. 4(h) and Fig. 5(h). Because the active power received at the MMC-2 decreases, the active power transferred from the MMC-1 also decreases at the same time to make a power balancing of the system (Fig. 5(h)). Finally, Figs. 4(i) and Fig. 5(i) present the capacitor voltages of the MMC-1.

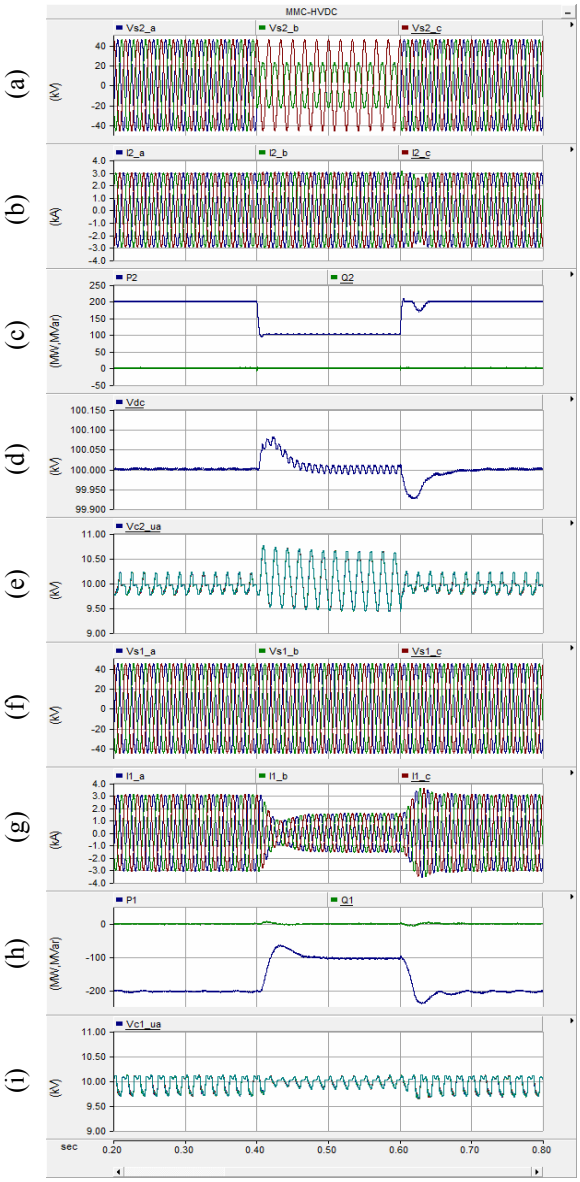

Fig. 5. The operation of the MMC-HVDC system with the PR current controllers under the single phase-to-ground fault: (a) MMC-2 three-phase voltages; (b) MMC-2 three-phase currents; (c) MMC-2 active and reactive powers, (d) dc-link voltage; (e) MMC-2 capacitor voltages; (f) MMC-1 three-phase voltages; (g) MMC-1 three-phase currents; (h) MMC-1 active and reactive powers; (i) MMC-1 capacitor voltages.

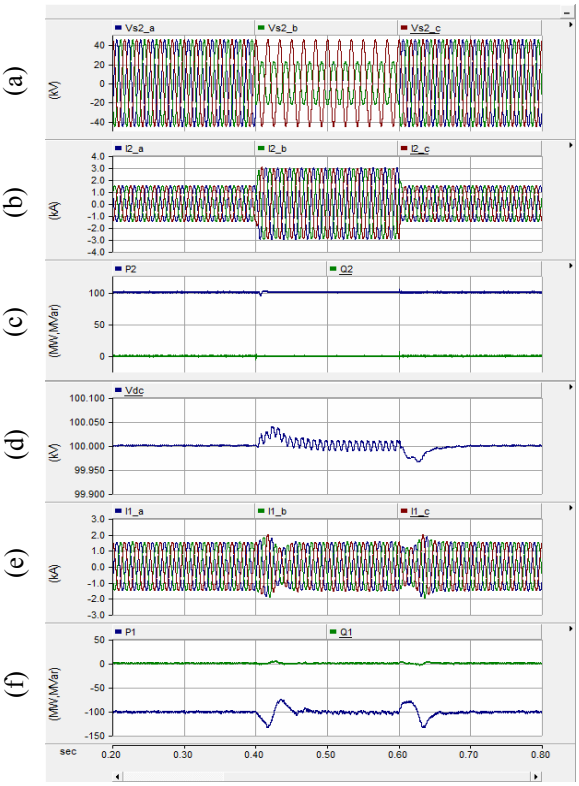

Fig. 6. The adjusting ability of the PR current controllers: (a) MMC-2 three-phase voltages; (b) MMC-2 three-phase currents; (c) MMC-2 active and reactive powers; (d) dc-link voltage; (e) MMC-1 three-phase currents; (f) MMC-1 active and reactive powers.

Table 1. Parameters of the MMC-HVDC system

Quantity	Value
Active power	200 MW
AC system voltage	154 kV
Nominal frequency	60 Hz
Transformer ratio	154 kV/55.1135 kV
dc-link voltage	±50 kV
Number of SMs per arm	10
MMC switching frequency	5 kHz
Sub-module capacitor	3300 μF

To evaluate a more convincingly the control ability of the PR current controllers under the unbalanced voltage conditions, another simulation is set up. In this case, the command active power is set at 100 MW. The simulation results are shown in Fig. 6. The SPG fault occurs at 0.4 s and restores at 0.6 s as shown in Fig. 6(a). During faults, the PR current controllers control the currents to the reference value to get the command power or at least to get the maximum net power as depicted in Figs. 6(b)-(c). As seen in Fig. 6(c), the active power reaches its command value during the SPG fault. Fig. 6(d) shows the dc-link voltage, it has a very small oscillation. The three-phase currents and the active and reactive powers of the MMC-1 are expressed in Figs. 6(e)-(f).

5. Conclusions

This paper presents an application of the PR controller in the MMC-HVDC system under the unbalanced voltage conditions. With the PR controller, the complicated analysis of the positive and negative sequence components in the dq-frame is not necessary. The currents are controlled directly in the αβ-frame. The simulation results have demonstrated that the ac currents are kept balanced and the dc-link voltage is constant under the unbalanced voltage conditions. Besides, the adjusting ability of the PR current controllers to get the command power or the maximum power has been also confirmed.

Acknowledgements

This work was supported by the Development of 20MW VSC HVDC for offshore wind-farm interconnection of the Korea Institute of Energy Technology Evaluation and Planning (KETEP), granted financial resource from the Ministry of Trade, Industry & Energy, Republic of Korea. (*No. 2012T100201551*).

This work was supported by the Expansion of the Type Testing Site for Wind Turbines *(NO.2012T100201731)* of the Korea Institute of Energy Technology Evaluation and Planning (KETEP) grant funded by the Korea government Ministry of Trade, Industry and Energy.

References

[1] S. Allebrod, R. Hamerski, and R. Marquardt, "New Transformerless, Scalable Modular Multilevel Converters for HVDC-Transmission," *IEEE Power Electronics Specialists Conference*, PESC 2008, pp. 174-179, 2008.

[2] S. Rohner, S. Bernet, M. Hiller, and R. Sommer, "Modulation, Losses, and Semiconductor Requirements of Modular Multilevel Converters," *IEEE Transactions on Industrial Electronics*, vol. 57, no. 8, pp. 2633-2642, Aug. 2010.

[3] M. Hagiwara and H. Akagi, "Control and Experiment of Pulsewidth-Modulated Modular Multilevel Converters," *IEEE Transactions on Power Electronics*, vol. 24, no. 7, pp. 1737-1746, July 2009.

[4] Jiangchao Qin and Maryam Saeedifard, "Predictive Control of a Modular Multilevel Converter for a Back-to-Back HVDC System," *IEEE Transaction on Power Delivery*, vol. 27, no. 3, pp. 1538-1547, July 2012.

[5] Qingrui Tu, Zheng Xu, and Lie Xu, "Reduced Switching-Frequency Modulation and Circulating Current Suppression for Modular Multilevel Converters," *IEEE Transactions on Power Delivery*, vol. 26, no. 3, pp. 2009-2017, July 2011.

[6] M. Saeedifard and R. Iravani, "Dynamic Performance of a Modular Multilevel Back-to-Back HVDC System," *IEEE Transactions on Power Delivery*, vol. 25, no. 4, pp. 2903-2912, Oct. 2010.

[7] Minyuan Guan and Zheng Xu, "Modeling and Control of a Modular Multilevel Converter-Based HVDC System under Unbalanced Grid Conditions," *IEEE Transactions on Power Electronics*, vol. 27, no. 12, pp. 4858-4867, Dec. 2012.

[8] Qingrui Tu, Zheng Xu, Young Chang, and Li Guan, "Suppressing DC Voltage Ripples of MMC-HVDC under Unbalanced Grid Conditions," *IEEE Transactions on Power Delivery*, vol. 27, no. 3, pp. 1332-1338, July 2012.

[9] Qingrui Tu, Zheng Xu, Young Chang, and Li Guan, "Suppressing DC Voltage Ripples of MMC-HVDC System under Unbalanced Grid Conditions," *IEEE Transactions on Power Delivery*, vol. 27, no. 3, pp. 1332-1338, July 2012.

[10] Lie Xu and Yi Yang, "Dynamic Modeling and Control of DFIG-Based Wind Turbines under Unbalanced Network Conditions," *IEEE Transactions on Power Systems*, vol. 22, no. 1, pp. 314-323, Feb. 2007.

[11] R. Teodorescu, F. Blaabjerg, M. Liserre, and P. C. Loh, "Proportional-Resonant Controllers and Filters for Grid-Connected Voltage-Source Converters," *in IEE Proceedings Electric Power Applications,* vol. 153, no. 5, pp. 750-762, 2006.

Ngoc-Thinh Quach He received a B.S. degree in Electrical Engineering from Can Tho University, Vietnam, in 2007 and a M.S. degree in Electrical Engineering from Jeju National University, S. Korea, in 2012. He is currently a PhD candidate in the Department of Electrical Engineering, Jeju National University, S. Korea. His research interests include wind energy systems, HVDC systems, and power system stability.

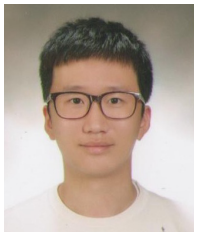

Ji-Han Ko He received a B.S. degree in Electrical Engineering from Jeju National University, S. Korea, in 2012. He is currently a M.S. student in the Multidisciplinary Graduate School Program for Wind Energy, Jeju National University, S. Korea. His research interests include wind energy systems, HVDC system, and power electronics.

Dong-Wan Kim He received a B.S. degree in Electrical Engineering from Jeju National University, S. Korea, in 2012. He is currently a M.S. student in the Multidisciplinary Graduate School Program for Wind Energy, Jeju National University, S. Korea. His research interests include wind energy systems, micro grid, and power electronics.

Eel-Hwan Kim He received his B.S., M.S. and Ph.D. degrees in Electrical Engineering from Chung-Ang University, Seoul, Korea, in 1985, 1987 and 1991, respectively. Since 1991, he has been with the Department of Electrical Engineering, Jeju National University in Jeju, Korea, where he is currently a professor. He was a Visiting Scholar at the Ohio State University in 1995 and University of Washington in 2004. His research activities are in the area of power electronics and control, which includes the drive system, renewable energy control applications, and power quality. He is a member of KIEE, KIPE, and IEEE.